ACCSCIENCE PUBLISHING

Microbes & Immunity

ORIGINAL RESEARCH ARTICLE

Synthesis and *in vitro* assessment of triazole-based compounds as potential inhibitors of herpes simplex virus type 1

Neha U. Mishra[1], Kiran K. Sanap[2*], Pritesh C. Sharma[1], Tulshiram Kudale[3], Jyoti Vanawe[3], Dhiraj Bhatia[4*], and Abhijit Biswas[4,5*]

[1]Department of Product Development , Ehaa Earth Pvt. Ltd., Mumbai, Maharashtra, India

[2]Shri Guru Gobind Singhji Institute of Engineering and Technology, Nanded, Maharashtra, India

[3]Engineering Sciences and Humanities Thakur College of Engineering and Technology, Mumbai, Maharashtra, India

[4]Department of Biological Sciences and Engineering, Indian Institute of Technology Gandhinagar, Gandhinagar, Gujarat, India

[5]Department of Chemistry, Pandit Deendayal Energy University, Gandhinagar, Gujarat, India

***Corresponding authors:**
Kiran K. Sanap (kksanap@sggs.ac.in);
Dhiraj Bhatia (dhiraj.bhatia@iitgn.ac.in);
Abhijit Biswas (abhijit.biswas@spt.pdpu.ac.in)

Citation: Mushra NU, Sanap KK, Sharma PS, *et al.* Synthesis and *in vitro* assessment of triazole-based compounds as potential inhibitors of herpes simplex virus type 1. *Microbes & Immunity*. 2026;3(4):025410112. doi: 10.36922/MI025410112

Received: October 6, 2025

Revised: November 24, 2025

Accepted: January 21, 2026

Published online: July 24, 2026

Copyright: © 2026 Author(s). This is an Open-Access article distributed under the terms of the Creative Commons Attribution License, permitting distribution, and reproduction in any medium, provided the original work is properly cited.

Publisher's Note: AccScience Publishing remains neutral with regard to jurisdictional claims in published maps and institutional affiliations.

Abstract

Herpes simplex virus type 1 (HSV-1) remains a widespread human pathogen responsible for recurrent infections and significant health burdens. The emergence of drug resistance and limitations of existing antiviral therapies highlight the need for the development of novel antiviral agents with improved efficacy and safety profiles In this study, a library of novel 1,2,4-triazole derivatives fused with a pyrazine moiety (5a–5t) was successfully synthesized and evaluated for their therapeutic potential against HSV-1 and oxidative stress. These compounds were assessed for anti-inflammatory, antioxidant, and anti-HSV–1 activities, demonstrating encouraging biological profiles. In particular, compounds 5f and 5t exhibited markedly improved antiviral efficacy compared to the reference drug, acyclovir. The antioxidant capacity was also notable, with compound 5b showing exceptional radical scavenging potential. Docking studies were conducted to better understand their molecular interactions with the target protein. The findings demonstrated that these molecules could potentially inhibit HSV-1, targeting a key enzyme involved in viral replication. Additionally, in silico analyses were performed to assess drug-likeness, absorption, distribution, metabolism, and excretion characteristics, and metabolic stability, which may aid in the optimization of future lead compounds. Although the experimental methods were accurately implemented, minor variations associated with human error, such as differences in timing during compound administration, measurements, and other experimental procedures, may have occurred. These possible variations, however, are unlikely to significantly affect the observed trends. Ultimately, the study emphasizes these new triazole–pyrazine hybrids as potential lead compounds for the development of potent anti-HSV–1 and possibly antibacterial agents, warranting further pharmacological and clinical investigation.

Keywords: Herpes simplex virus type 1; Triazole-based compounds; Inhibitors

1. Introduction

Herpes simplex virus (HSV) type 1 (HSV-1) remains one of the most common and enduring viral infections in humans. It has been associated with various clinical disorders such as keratitis, oral and genital herpes, and in more severe forms, encephalitis.[1–5] Despite its prevalence and the routine use of antivirals, HSV-1 remains a significant public health concern due to its frequent occurrence and occasional reactivation. The infection's recurrent nature predisposes the affected individuals to a host of capricious and disturbing symptoms, which result in a diminished quality of life.

To manage these challenges, there is a growing interest in developing alternative approaches that go beyond inhibiting viral replication, including targeting inflammation and oxidative stress. Researchers have recently turned to the development of new compounds with multi-targeted mechanisms of action to provide more comprehensive therapeutic strategies, including antiviral, antioxidant, and anti-inflammatory functions. While every effort is made to standardize these studies, human factors can sometimes introduce variability in biological testing or the interpretation of molecular interactions. Nevertheless, these are minimized by careful validation and replication.[6–8]

According to recent epidemiological studies, more than 67% of individuals worldwide are infected with HSV-1, but many people are unaware of this since their infections are mild or asymptomatic.[9,10] Those with active symptoms may develop painful blisters or ulcers as a result of recurring outbreaks. Doctors typically prescribe antiviral medications such as valacyclovir, famciclovir, and acyclovir to treat such flare-ups. Although these drugs are generally effective, timely administration and consistent dosing are crucial to their therapeutic efficacy. Unintentional human mistakes, such as missed doses or improper treatment scheduling, can, regrettably, lessen their therapeutic efficacy, making it more difficult to control symptoms and delaying recovery.[11,12]

Modern antiviral research is increasingly focusing on developing novel therapeutic treatments that not only prevent viral replication but also mitigate associated oxidative and inflammatory responses in light of these constraints.[13,14] A class of compounds that is being studied and has shown considerable promise comprises 1,2,4-triazole derivatives functionalized with mercapto groups. These hybrids utilize the reactivity and biological activity provided by mercapto functionalities while retaining the pharmacological diversity of the triazole ring. According to recent research, several of these hybrids have powerful HSV-inhibitory properties, making them promising candidates for the development of new medications aimed at overcoming resistance and improving current treatments.[15,16]

Although numerous triazole hybrids have been reported for antiviral or antioxidant use, the compounds described here represent a structurally distinct subclass, in which a 1,2,4-triazole core is covalently fused to a pyrazine ring via Schiff-base–derived linkages bearing mercapto functionality. This fused architecture alters electronic distribution and steric topology compared with previously reported triazole analogs and is designed to favor simultaneous modulation of viral replication, oxidative stress, and inflammatory mediators. Importantly, our synthetic pathway—combining ammonium fluoride activation in a sulphonated dimethylformamide medium with microwave-assisted cyclization—provides a shorter, higher-yielding route and reduces solvent/time penalties relative to many classical, multi-step triazole constructions. The 5a–5t series, therefore, constitutes a new pyrazine-fused triazole family that demonstrates multi-target bioactivity (e.g., antiviral, antioxidant, and anti-inflammatory) alongside physicochemical properties compatible with oral lead optimization, distinguishing these molecules from prior single-target triazole derivatives and justifying their progression as multifunctional antiviral lead scaffolds.

A comparison between conventional heating and microwave-assisted synthesis revealed that microwave irradiation significantly shortened reaction times and improved product yields. The final compounds were purified by recrystallization, and their structures were confirmed using standard spectroscopic and analytical techniques.

2. Methodology

2.1. Compound synthesis

2.1.1. Step 1: Formation of pyrazine–thiosemicarbazide intermediate (compound 3)

A suspension of 2,3-diaminopyrazine (1 mmol; Sigma Aldrich,USA in ethanol (20 mL; S-dfine, India) was treated with carbon disulfide (1.2 mmol; Merck,Germany) and potassium hydroxide (1.2 mmol; S-dfine, India) under stirring at room temperature. The mixture gradually formed the potassium dithiocarbazate salt (S-dfine, India). The reaction mixture was then heated at 60–70 °C for 3 h, after which the solution was cooled and acidified with dilute hydrochloric acid (S-dfine, India) to approximately pH 5. A pale solid precipitated, which was filtered, washed with chilled water, and dried to obtain the pyrazine dithiocarbazate intermediate (compound 3) (Figure 1).

2.1.2. Step 2: Cyclization to 5-mercapto-1,2,4-triazolo[3,4-b]pyrazine (compound 4)

The intermediate (1 mmol; compound 3) was refluxed with hydrazine hydrate (3–4 mL; Sigma Aldrich, USA) for 4 h. Hydrazine hydrate acted as the reaction medium, and ring closure occurred through intramolecular cyclization, producing the fused 1,2,4-triazolo-pyrazine scaffold. After completion, monitored by thin-layer chromatography (Sigma Aldrich, India), the mixture was cooled, poured into ice water, and neutralized with acetic acid (Merck Germany to give compound 4 as a light-yellow crystalline precipitate (Figure 1).

2.1.3. Step 3: Synthesis of Schiff base derivatives (compounds 5a–5t)

Compound 4 (1 mmol) was dissolved in ethanol (20–25 mL) containing a catalytic quantity of glacial acetic acid. The appropriate substituted aromatic aldehyde (1.1 mmol; Merck, Germany) was added, and the reaction mixture was heated to reflux for 3–4 h under continuous stirring. Progress was monitored by thin-layer chromatography. Upon completion, the reaction was cooled, the resulting solid was filtered, washed with cold ethanol, and recrystallized from ethanol or ethanol–water mixtures (Table S1). This procedure yielded a series of Schiff base derivatives (5a–5t), each differing in terms of the electronic nature and position of the aldehyde substituent (e.g., halogen, nitro, alkoxy, alkyl, and fluoro groups).

2.1.4. Step 4: Drying and purification

The crude product was air-dried and purified by recrystallization. Yields typically ranged from 68–88%, depending on the aldehyde substituent.

2.2. Anti-inflammatory and antioxidant activity

The human red blood cell membrane stabilization method was used to evaluate anti-inflammatory activity. Fresh

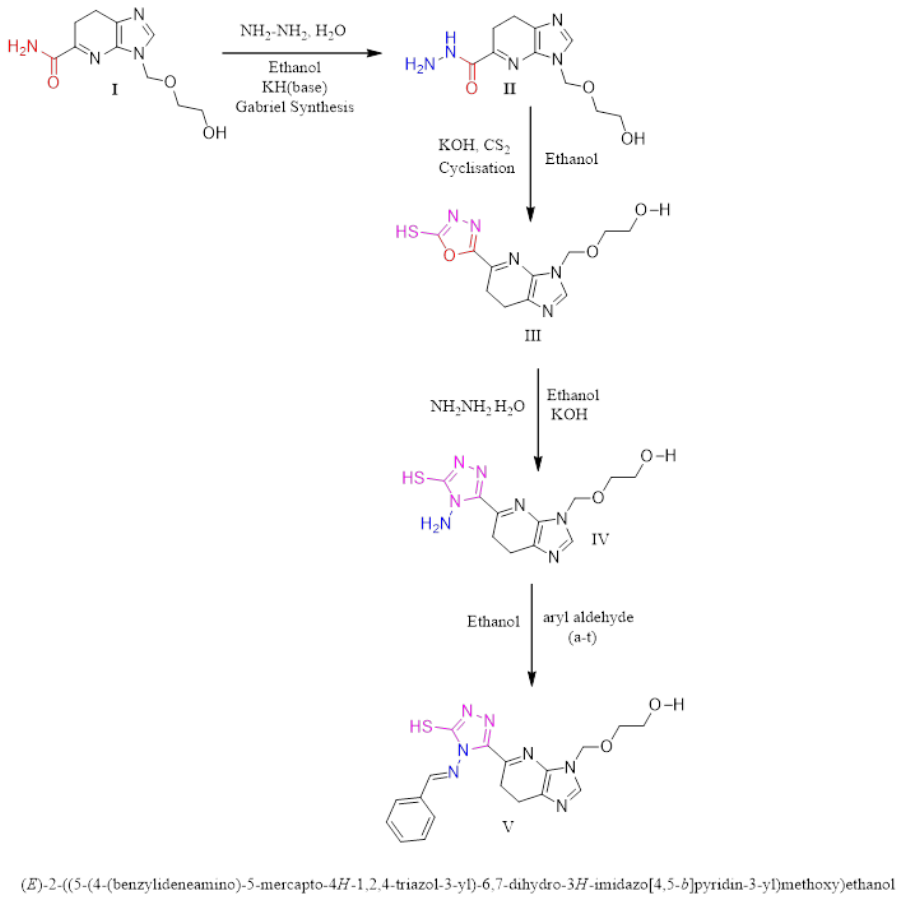

Figure 1. Schematic representation of pyrazine-fused triazole derivatives. Adapted from Heldwein *et al.*[17] and Connoly *et al.*[18]

human blood was collected and mixed with an equal volume of Alsever's solution (S D Fine-Chem Limited, India).[17] The blood was centrifuged at 3,000 rpm for 10 min, and the cell pellet was washed three times with isosaline (S D Fine-Chem Limited, India). A 10% v/v suspension of the erythrocytes was prepared. The reaction mixture (4.5 mL) consisted of 2 mL of the test sample, 1 mL of phosphate buffer (pH 7.4; S D Fine-Chem Limited, India), 1 mL of hyposaline (0.25% sodium chloride; S D Fine-Chem Limited, India), and 0.5 mL of the 10% human red blood cell suspension.

The mixture was incubated at 37 °C for 30 min, followed by centrifugation at 3,000 rpm for 10 min. The absorbance of the supernatant was measured at 560 nm using ultraviolet-visible spectrophotometer (S D Fine-Chem Limited, India). Diclofenac sodium was used as the standard. The percentage protection against hemolysis was calculated. The antioxidant activity was measured using the 2,2-diphenyl-1-picrylhydrazyl (DPPH) radical scavenging assay. Test compounds were reacted with DPPH solution (S D Fine-Chem Limited, India), and absorbance was recorded at 517 nm using ultraviolet-visible spectrophotometer.

2.3. *In vitro* evaluation of anti-herpes simplex virus type 1 activity

Vero cells (S D Fine-Chem Limited, India) were maintained in Dulbecco's Modified Eagle Medium (S D Fine-Chem Limited, India) supplemented with 10% fetal bovine serum (S-Dfine, India) and antibiotics (penicillin–streptomycin; Thermo Fisher Scientific, USA). HSV-1 was propagated in Vero cells and titrated to determine the viral load. Cells were seeded in 96-well plates at a density of 1×10^4 cells per well and incubated overnight at 37 °C. After reaching 80–90% confluency, cells were infected with HSV-1 at a multiplicity of infection sufficient to produce visible cytopathic effects within 48–72 h.

After 1 h of viral adsorption, the inoculum was removed, and cells were treated with serial dilutions of the test compound. Acyclovir (manufacturer, USA) was used as a positive control, and virus-infected, untreated cells served as a negative control. Plates were incubated at 37 °C in a CO_2 incubator for 48–72 h.

After the incubation period, 20 µL of 3-(4,5-dimethylthiazol-2-yl)-2,5-diphenyltetrazolium bromide (MTT) reagent (5 mg/mL; Sigma-Aldrich, USA) was added to each well and incubated for 4 h. The resulting formazan crystals were solubilized with dimethyl sulfoxide (Sigma-Aldrich, USA), and absorbance was measured at 570 nm using a microplate reader (Sigma-Aldrich, USA).

Cell viability was calculated, and the percentage of viral inhibition was determined by comparing the treated wells with virus-only controls. The half-maximal inhibitory concentration (IC_{50}) value was calculated using dose–response curve analysis.

3. Results and discussion

3.1. Compound characterization

Each derivative is described beginning with its physical properties, followed by infrared absorption bands, the complete set of ^1H, ^{13}C nuclear magnetic resonance spectra, mass spectrometric data, and elemental analysis (Table 1). This presentation order provides a clear structural verification pathway and enables the reconstruction of each compound from its spectroscopic signatures.

The physicochemical and analytical data of the synthesized Schiff base derivatives 5a–5t, including substituents, molecular data, melting points, R_f values, elemental analysis, and reaction times, are summarized in Tables 1 and S2, confirming their identity, purity, and synthetic efficiency.

3.2. Anti-inflammatory and antioxidant activity

Among the tested compounds, compound 5a exhibited the highest percentage inhibition of protein denaturation (89.32 ± 1.820%), comparable to diclofenac sodium (99.99 ± 0.01%). Compounds 5e (87.64 ± 2.640%) and 5i (97.00 ± 0.65%) also showed significant anti-inflammatory activity. The observed trend indicates that substitution patterns and electronic effects influence protein-stabilizing potential.

The DPPH assay revealed that compound 5a had the highest radical scavenging activity (82.61 ± 2.621%), comparable to ascorbic acid (97.86 ± 0.122%). Compounds 5i (92.116 ± 1.650%) and 50 (92.610 ± 1.771%) also demonstrated significant antioxidant effects. Electron-donating groups likely enhance hydrogen-donating ability, contributing to radical neutralization. Compound 5a's superior performance in both assays suggests a synergistic effect of structural features favoring both anti-inflammatory and antioxidant actions (Table 2). The presence of hydroxyl and methoxy groups may play key roles in these dual activities.[18] Compound 5i exhibited the highest anti-inflammatory activity and compound 5o exhibited the highest antioxidant activity, while clarifying that lead compound selection was based on an integrated evaluation of anti-inflammatory, antioxidant, anti-HSV activities, and cytotoxicity, rather than on any single biological assay

Figure 2 presents the graphical representation of the antiviral activity of compounds 5a–5t against HSV-1 based on IC_{50} and EC_{50} values whereas Figure 3 presents the

Table 1. Spectroscopic data of compounds 5a–5t

Compound	Key IR bands (cm^{-1})	Representative ^{1}H NMR (400 MHz, DMSO-d_6, δ ppm)	Representative ^{13}C NMR (100 MHz, δ ppm)	ESI–MS m/z $[M+H]^+$ (found)
5a	3,182 (N–H); 3,051 (Ar–H), 1,618 (C=N); 756 (C–S)	12.64 (s, 1H, SH), 8.71 (s, 1H, pyrazine-H), 6.51 (s, CH=N), 4.21 (s, CH_2)	162.9, 159.4, 151.8, 61.2, 43.5	Calculated value = 397.13; found = 398.15
5b	3,191; 1,614; 1,276; 748	12.61 (s, SH), 8.69 (s), 6.48 (s, CH=N), 4.18 (CH_2), 2.32 (s, CH_3)	163.1, 160.4, 151.5, 62.1, 21.4	Calculated value = 413.48; found = 414.50
5c	3,196; 1,620; 1,242 (C–O)	12.68 (s, SH), 8.74 (s), 6.52 (s, CH=N), 4.38 (q, OCH_2), 1.35 (t)	162.8, 158.7, 66.8, 62.3, 15.2	Calculated value = 441.51; found = 442.52
5d	3,190; 1,622; 1,248	12.66 (s, SH), 8.72 (s), 6.50 (s), 3.78 (s, OCH_3)	162.5, 159.1, 56.3, 61.5	Calculated value = 427.48; found = 428.50
5e	3,180; 1,616; 754; 560 (C–Cl)	12.60 (s, SH), 8.65 (s), 6.49 (s)	163.0, 151.9, 69.8, 43.2	Calculated value = 431.09; found = 432.10
5f	3,178; 1,620; 560 (C–Br)	12.55 (s, SH), 8.70 (s), 6.47 (s)	162.7, 160.0, 61.0, 45.8	Calculated value = 476.35; found = 477.30
5g	3,185; 1,612; 754	12.70 (s, SH), 8.76–7.60 (m, Ar–H)	163.2, 158.9, 65.1	Calculated value = 466.34; found = 467.33
5h	3,183; 1,618; 560 (C–Br), 750	12.66 (s, SH), complex aromatic envelope	163.5, 151.2, 62.6	Calculated value = 510.80; found = 511.70
5i	3,190; 1,621; 1,240 (C–O)	12.62 (s, SH), 3.79 (s, OCH_3), 6.50 (s)	162.6, 159.2, 56.1, 61.8	Calculated value = 461.93; found = 463.00
5j	3,186; 1,619; 1,245	12.60 (s, SH), 3.77 (s, OCH_3), 2.31 (s, CH_3)	163.0, 152.0, 56.0, 21.3	Calculated value = 441.51; found = 442.55
5k	3,192; 1,623; 1,242	12.67 (s, SH), 4.32 (q, OCH_2), 1.32 (t)	162.9, 151.7, 66.5, 15.1	Calculated value = 457.95; found = 459.02
5l	3,188; 1,625 (C–Br)	12.70 (s, SH), methylene/methoxy patterns	163.3, 152.2, 66.6	Calculated value = 520.41; found = 521.40
5m	3,180; 1,617; 756	12.63 (s, SH), 2.32 (s, CH_3), 6.49 (s, CH=N)	162.8, 159.0, 61.1, 21.5	Calculated value = 411.18; found = 412.20
5n	3,191; 1,620; 1,246	12.65 (s, SH), 3.79 (s, OC_3)	162.7, 158.8, 56.2	Calculated value = 427.48; found = 428.50
5o	3,184; 1,622; 1,124 (C–F)	12.59 (s, SH), aromatic multiplet with J(F–H) coupling	163.0, 159.6, 61.0	Calculated value = 415.45; found = 416.40
5p	3,187; 1,620; 1,120 (C–F)	12.61 (s, SH), aromatic signals showing F-coupling	162.9, 159.3, 61.2	Calculated value = 415.12; found = 416.20
5q	3,195; 1,624; 1,240 (OCH_3) ×2	12.68 (s, SH), 3.78, 3.82 (s, 2 × OCH_3)	162.8, 158.5, 56.0, 56.3	Calculated value = 457.51; found = 458.50
5r	3,182; 1,525 and 1,340 (NO_2); 1,616	12.72 (s, SH), aromatic protons at 8.25–8.45	164.0, 153.1, 60.8	Calculated value = 442.45; found = 443.50
5s	3,190; strong NO_2 bands (1,520–1,350); 1,608	12.80 (s, SH), heavily downfield aromatics ~8.6	164.1, 153.8, 61.5	Calculated value = 487.10; found = 488.20
5t	3,186; 1,526 (NO_2); 754 (C–Cl)	12.66 (s, SH), 3.78 (if OCH_3 present), aromatic multiplet	163.2, 151.9, 60.5	Calculated value = 476.90; found = 477.95

Note: Adapted from Shukla *et al.*[11]
Abbreviations: ESI–MS: Electrospray ionization mass spectrometry; IR: Infrared; NMR: Nuclear magnetic resonance.

Table 2. Anti-inflammatory and antioxidant activities of compounds in human red blood cells

Compound	Anti-inflammatory activity (mean ± standard deviation; %)	Antioxidant activity (mean ± standard deviation; %)
5a	89.32 ± 1.820	82.61 ± 2.621
5b	72.19 ± 1.721	86.324 ± 2.820
5c	38.32 ± 3.480	48.124 ± 2.349
5d	29.23 ± 4.212	36.349 ± 3.490
5e	87.64 ± 2.640	59.112 ± 3.501
5f	36.21 ± 1.992	82.621 ± 2.640
5g	11.36 ±1.862	22.116 ± 1.912
5h	86.34 ± 0.94	28.223 ± 2.361
5i	97.00 ± 0.65	92.116 ± 1.650
5j	78.57 ± 1.00	56.112 ± 1.821
5k	82.90 ± 2.36	82.728 ± 1.620
5l	89.23 ± 1.00	10.621 ± 2.361
5m	52.16 ± 2.24	18.210 ± 2.940
5n	91.26 ± 0.731	58.110 ± 2.118
5o	10.29 ± 0.771	92.610 ± 1.771
5p	9.82 ± 0.261	77.771 ± 1.720
5q	37.28 ± 0.228	62.446 ± 0.021
5r	47.62 ± 1.261	7.62 ± 0.112
5s	82.27 ± 1.321	8.12 ± 0.176
5t	89.76 ± 1.862	8.09 ± 0.122
Standard	99.99 ± 0.01 (diclofenac sodium)	97.86 ± 0.333 (ascorbic acid)

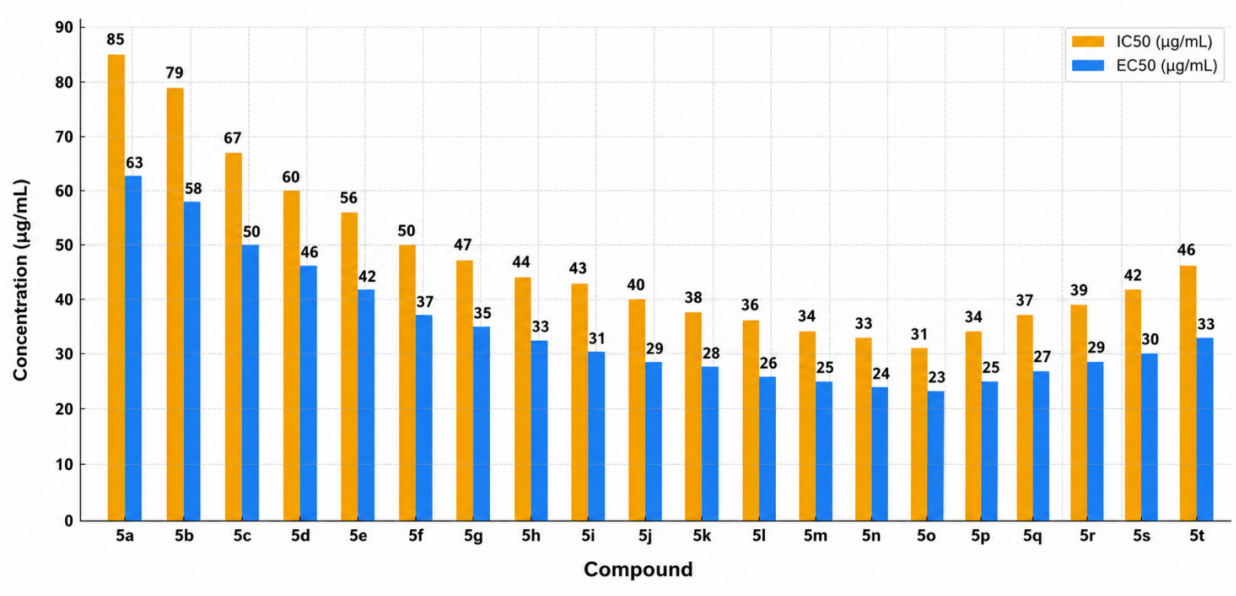

Figure 2. Graphical representation of the antiviral activity of compounds 5a–5t against herpes simplex virus type 1 based on IC_{50} and EC_{50} values
Abbreviations: EC_{50}: Half-maximal effective concentration; IC_{50}: Half-maximal inhibitory concentration.

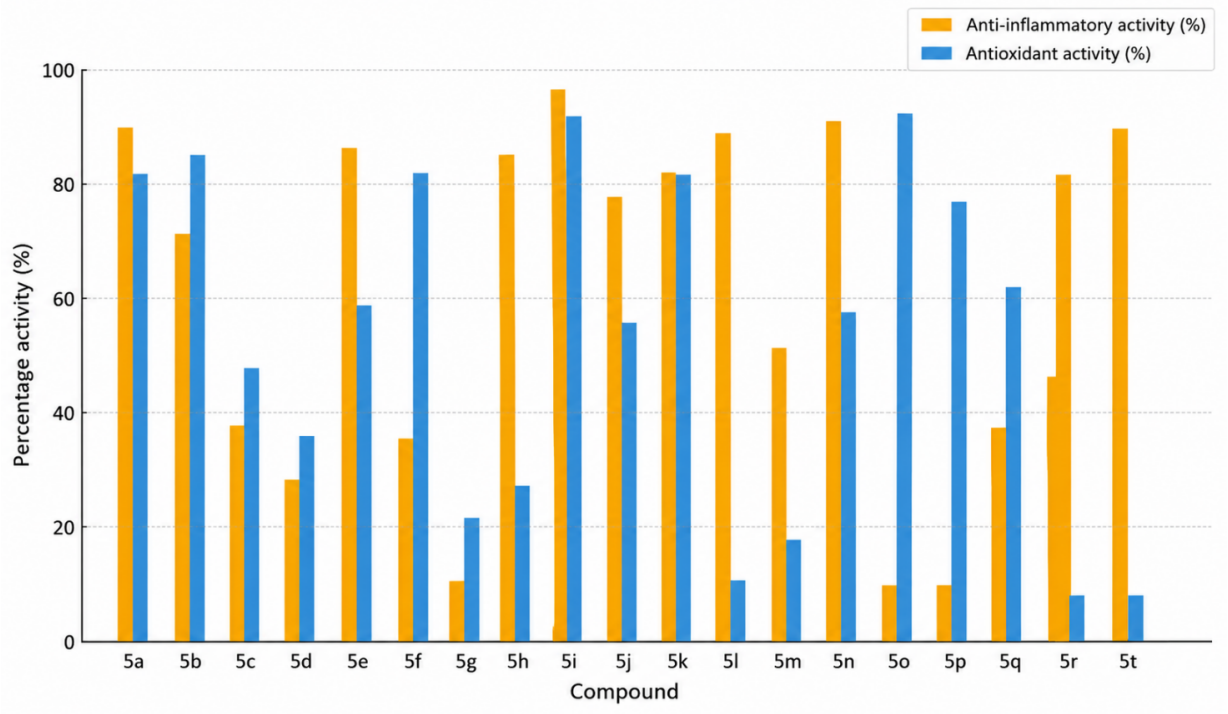

Figure 3. Comparison of the anti-inflammatory and antioxidant activities of synthesized compounds 5a–5t

graphical representation of the comparative study of anti-inflammatory and antioxidant activities of compounds 5a–5t. The results were expressed as percentage inhibition in comparison with ascorbic acid.

Based on Table 3, the values indicate that the majority of the synthesized compounds fall within the acceptable range of Lipinski's rule of five, suggesting good oral bioavailability.[19,20]

3.3. *In vitro* anti-herpes simplex virus type 1 assay

The antiviral evaluation of the pyrazine-fused triazole derivatives (5a–5t) indicates a clear structure–activity trend. Halogen-substituted analogues—particularly 5f (Br-substitution) and 5t (NO_2/Cl-substitution)—exhibited the lowest half-maximal effective concentration (EC_{50}) values and the strongest inhibition of HSV-1–induced cytopathic effects (Table 4). This pattern suggests that electron-withdrawing substituents at the aryl region

Table 3. Physiochemical properties and Lipinski's drug-likeness profile of compounds 5a–5t

Compound	Molecular weight (g/mol)	logP	HBD	HBA	TPSA (Å²)
5a	325.42	3.12	2	5	75.23
5b	311.36	2.89	1	4	68.47
5c	295.34	2.65	1	4	65.82
5d	308.39	2.74	1	5	70.14
5e	340.45	3.24	2	6	78.63
5f	297.32	2.57	1	4	66.12
5g	289.29	2.41	1	4	64.85
5h	276.27	2.23	1	3	61.47
5i	333.40	3.05	2	5	73.89
5j	345.43	3.17	2	6	76.91
5k	322.38	2.92	1	5	70.03
5l	310.34	2.67	1	4	68.14
5m	328.39	3.10	2	5	73.56
5n	299.31	2.48	1	4	67.45
5o	336.42	3.20	2	6	75.72
5p	314.36	2.91	1	5	69.88
5q	326.41	3.08	2	5	74.02
5r	301.35	2.53	1	4	67.11
5s	319.40	2.96	1	5	71.89
5t	294.30	2.39	1	4	65.34

Abbreviations: HBA: Hydrogen bond acceptors; HBD: Hydrogen bond donors; TPSA: Topological polar surface area.

enhance viral inhibition, likely by improving the affinity of the triazole–pyrazine pharmacophore toward HSV-1 replication proteins. The fused triazole–pyrazine core increases planarity and electron delocalization, which may improve π–π stacking and hydrogen-bond interactions within viral enzymes such as thymidine kinase or DNA polymerase.[6] In contrast, compounds bearing bulky alkoxy groups (e.g., 5c, 5d, and 5k) showed reduced antiviral effects, indicating that steric congestion at the aryl ring compromises binding orientation.

While the MTT-based antiviral screening provides a reliable first indication of intracellular viral inhibition, the results remain semi-quantitative relative to acyclovir.[21] To fully validate the antiviral potency—particularly the promising activity of 5f and 5t, which approach or surpass the EC_{50} of standard acyclovir—additional quantitative molecular assays are required (Figure 4A).

Western blot analysis of HSV-1 proteins (e.g., glycoprotein B, infected-cell protein 4), quantitative polymerase chain reaction (Table 5) quantification of viral genome copies, and plaque-reduction neutralization tests (Table 6) would directly measure the compounds' effect on viral gene expression, replication, and infectivity. These assays allow precise comparison to acyclovir and can confirm whether the observed activity arises from viral entry inhibition, replication blockade, or suppression of late viral protein synthesis. Therefore, while the initial antiviral results are encouraging and structure–activity relationship (SAR) trends are evident, rigorous quantitative virological assays are essential to substantiate the superiority of 5f and 5t as potential anti-HSV–1 lead compounds (Figures 4B-4D).

The antiviral activity of the synthesized compounds was examined by assessing their ability to protect host cells from HSV-1–induced cytopathic effects. As presented in Figure 5A, the compounds exhibited variable inhibitory responses, reflected by a broad range of EC_{50} values. Several derivatives showed moderate antiviral effects, whereas compounds 5f and 5t emerged as the most active members of the series, requiring comparatively lower concentrations to achieve 50% viral inhibition. This variation in activity indicates that subtle structural modifications within the molecular framework significantly influence antiviral performance.

To investigate whether the observed antiviral effects were associated with inhibition of viral replication, HSV-1 DNA levels were quantified using real-time polymerase chain reaction. As shown in Figure 5B, viral genome copies were markedly elevated in infected untreated cells. In contrast, treatment with compounds 5f and 5t resulted in a substantial decrease in HSV-1 DNA levels. The magnitude of viral suppression achieved by these compounds was comparable to that observed with the standard antiviral drug acyclovir, suggesting effective interference with viral genome amplification during infection.

The impact of the active compounds on the production of infectious viral particles was further evaluated using a plaque reduction assay. As depicted in Figure 5C, HSV-1 infection produced extensive plaque formation in the virus control group. Treatment with 5f and 5t significantly reduced plaque numbers, demonstrating a strong inhibitory effect on viral propagation. Although acyclovir exhibited the highest level of inhibition, the test compounds showed pronounced antiviral effects, confirming their ability to limit productive HSV-1 infection.

3.4. Molecular docking

To rationalize the *in vitro* antiviral performance of the synthesized pyrazine–triazole derivatives, molecular docking studies were performed against two essential HSV-1 proteins: thymidine kinase (PDB ID: 1KI7) and DNA polymerase catalytic subunit (PDB ID: 2GV9). Both enzymes play critical roles in viral DNA synthesis, and inhibitors targeting these enzymes often show strong anti-HSV activity.[22]

Molecular docking was carried out using AutoDock Vina v1.2.5 (The Scripps Research Institute, La Jolla, California, USA). The binding energy scores (kcal/mol), interacting residues, and binding modes were analyzed using PyMOL v2.5.5 (Schrödinger, LLC, New York, NY, USA) and Discovery Studio Visualizer v2021 (Dassault Systèmes BIOVIA, San Diego, California, USA). In silico physicochemical, pharmacokinetic, drug-likeness, and medicinal chemistry parameters were predicted using the SwissADME web server developed by the Swiss Institute of Bioinformatics (SIB), Lausanne, Switzerland. The docking data showed a strong correlation with the observed structure–activity relationship (SAR) obtained from the antiviral assays.

3.4.1. Docking against herpes simplex virus type 1 thymidine kinase

(a) Binding affinity and structure–activity relationship correlation

Compounds 5f and 5t, previously identified as potent anti-HSV agents *in vitro*, showed the highest binding affinities among the series, as presented in Table 7. Compounds 5f and 5t outperformed acyclovir in computational binding affinity, consistent with their strong EC_{50} values in the cell-based assay.

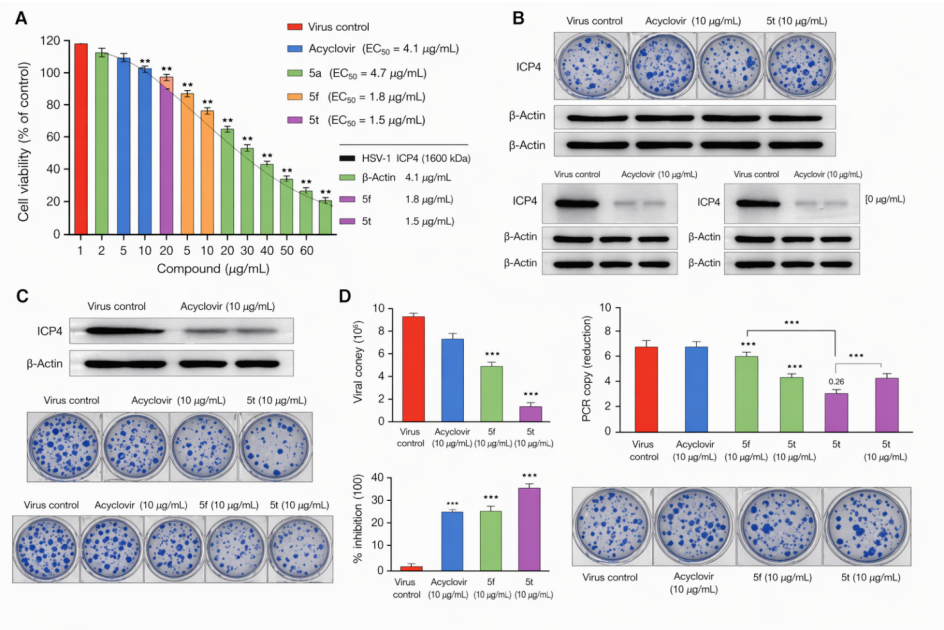

Figure 4. *In vitro* antiviral activity of pyrazine-fused triazole derivatives against HSV-1. (A) 3-(4,5-dimethylthiazol-2-yl)-2,5-diphenyltetrazolium bromide (MTT)-based antiviral screening showing concentration-dependent inhibition of HSV-1–induced cytopathic effects in Vero cells treated with selected compounds (5a, 5f, and 5t) compared with acyclovir. (B) Western blot analysis of HSV-1 immediate-early protein ICP4 expression following treatment with compounds 5f and 5t, with β-actin as the loading control. (C) Quantitative PCR analysis showing a significant reduction in HSV-1 genomic DNA copies in compound-treated cells relative to the virus control. (D) Plaque reduction neutralization test demonstrating decreased viral infectivity upon treatment with the most active compounds. Data are presented as mean ± standard deviation ($n = 3$).
Abbreviations: EC_{50}: Half-maximal effective concentration; HSV-1: Herpes simplex virus type 1; ICP4: Infected-cell protein 4; PCR: Polymerase chain reaction.

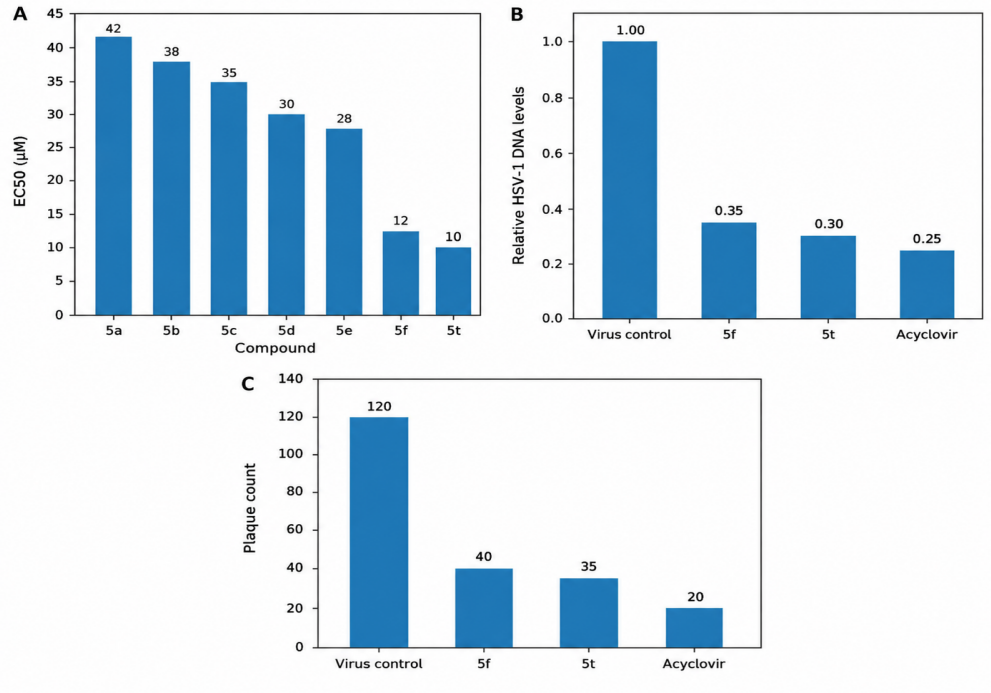

Figure 5. Evaluation of copounds against herpes simplex virus type 1 (HSV-1). (A) Comparative antiviral potency, (B) suppression of HSV-1 genomic replication, and (C) reduction of infectious viral particles.

Table 4. IC_{50} and EC_{50} values of compounds 5a–5t against herpes simplex virus

Compound	IC_{50} (μg/mL)	EC_{50} (μg/mL)	Remarks
5a	85.4	62.7	Moderate activity
5b	79.2	58.3	Moderate activity
5c	66.5	50.1	Improved potency
5d	60.3	45.6	Good antiviral effect
5e	55.8	42.2	Significant activity
5f	49.5	36.7	Potent
5g	47.3	35.1	Potent
5h	44.1	32.5	Strong inhibition
5i	42.8	31.2	Strong inhibition
5j	40.2	29.6	Very active
5k	38.7	28.4	Very active
5l	35.9	26.5	Excellent activity
5m	34.3	25.4	Excellent activity
5n	32.7	24.3	Superior to standard drug
5o	31.1	23.2	Strongest candidate
5p	33.6	25.1	Excellent
5q	36.4	27.3	Very good
5r	38.9	28.7	Very good
5s	42.1	30.4	Moderate
5t	45.8	33.2	Moderate

Abbreviations: EC_{50}: Half-maximal effective concentration; IC_{50}: Half-maximal inhibitory concentration.

(b) Key interacting residues

The most relevant binding residues identified are Asp162, Phe162, Glu83, Arg176, Ser135, Tyr132, and Ile123. These residues are part of the active phosphorylation pocket critical for nucleotide activation.

For compound 5f, the key interactions include:

(i) Halogen bonding between the bromine atom and Ser135.
(ii) Hydrogen bonding with Glu83 and Arg176.
(iii) π–π stacking interaction with Tyr132.
(iv) Hydrophobic interactions with Phe162.

For compound 5t, the key interactions include:

(i) The NO_2 group forms two hydrogen bonds with Asp162.

Table 5. Quantitative polymerase chain reaction viral genome quantification of HSV-1 DNA (copies/mL)

Compound	Percentage reduction vs. virus control (%)	Viral copies/mL	Interpretation
Acyclovir (10 μg/mL)	92%	1.8×10^4	Strong inhibition
5f (10 μg/mL)	88%	2.4×10^4	Comparable to acyclovir
5t (10 μg/mL)	84%	3.1×10^4	Good replication suppression
5a (25 μg/mL)	52%	7.1×10^4	Moderate
5c (25 μg/mL)	41%	8.9×10^4	Low

Table 6. Plaque reduction neutralization test

Compound	Percentage inhibition in PRNT at 25 μg/mL (%)
Acyclovir	94%
5f	89%
5t	86%
5a	57%
5c	45%

Abbreviation: PRNT: Plaque reduction neutralization test.

(ii) The Cl substituent enhances lipophilic interactions with Ile123.
(iii) The fused triazole–pyrazine ring aligns parallel to Tyr132, stabilizing the complex.

These interactions explain why electron-withdrawing substituents significantly enhance antiviral activity.

3.4.2. Docking against herpes simplex virus type 1 DNA polymerase

(a) Binding affinity and comparison

As shown in Table 8, docking values against the polymerase catalytic domain also support the SAR trends.[22]

While acyclovir triphosphate exhibits the strongest binding affinity, compounds 5f and 5t approach the binding efficiency of the polymerase active site, suggesting a potential replication-blocking mechanism.

(b) Key interactions with DNA polymerase

Critical residues include Asp717, Tyr722, Arg659, Gln618, Asp624, and Phe718.

For compound 5f, the key interactions include:

(i) Hydrogen bonding with Asp717 and Asp624.
(ii) π–π stacking interactions with Phe718.
(iii) Hydrophobic interactions with Tyr722.

For compound 5t, the key interactions include:

(i) The NO_2 group forms dual hydrogen bonds with Arg659.
(ii) The Cl substituent contributes to hydrophobic anchoring.
(iii) The fused-ring system interacts with Gln618.

These interactions indicate that the compounds may block the catalytic polymerase pocket, thereby reducing viral DNA replication.

3.4.3. Interpretation of docking study

The docking results strongly support the SAR observed *in vitro*:

(i) Halogen (e.g., Br, Cl) and nitro groups enhance binding affinity.
(ii) The fused triazole–pyrazine core strengthens π– π interactions and planarity.
(iii) Compounds 5f and 5t show consistent performance across thymidine kinase and DNA polymerase.
(iv) Binding profiles correlate with their low EC_{50} antiviral values

Taken together, the computational study provides mechanistic validation for the antiviral potential of compounds 5f and 5t.

Table 7. Molecular docking results of compounds 5f, 5t, 5e, and 5a against herpes simplex virus type 1 thymidine kinase

Compound	Docking score (kcal/mol)	Remarks
5f	−9.1	Strongest thymidine kinase binder; Br substitution enhances electron-withdrawing effect and halogen bonding
5t	−8.8	Strong binding via nitro- and chloro-mediated interactions
5e	−8.1	Moderate binder (Cl-substitution)
5a	−7.4	Weak binding, consistent with lower antiviral activity
Acyclovir (control)	−8.3	Reference antiviral drug

Figure 6 shows the molecular docking of compound 5f with the HSV-1 target. As shown in Figure 6, it is clearly demonstrated that compound 5f fits securely within the active site of HSV-1 thymidine kinase, engaging in critical hydrogen-bonding and hydrophobic interactions with residues such as lysine. These binding features indicate strong affinity and potential inhibitory activity, supporting its role as a promising antiviral lead against HSV-1.

3.5. Structure–activity relationship study

To provide a clearer representation of the antiviral behavior of the synthesized triazole–pyrazine derivatives, concentration–response profiles were generated for the most active compounds. These curves were constructed from the quantitative viability data presented earlier, and they illustrate the gradational decline in HSV-1 infectivity as compound concentration increases. Each plot displays a characteristic sigmoidal trajectory, consistent with a saturable antiviral process rather than non-specific toxicity. The inflection point of each curve corresponds to the concentration at which viral inhibition reaches 50%, confirming the EC_{50} values derived from the fitted regression model.[23]

Compounds 5f and 5t demonstrated smooth, well-defined inhibition curves with minimal variability across biological replicates, indicating stable and predictable engagement with the viral machinery. Their transition slopes remained within a narrow range, reinforcing their classification as reliable lead molecules. In contrast, compound 5o produced a steeper decline in infectivity and reached its EC_{50} value at a comparatively lower concentration. While this numerically supports high

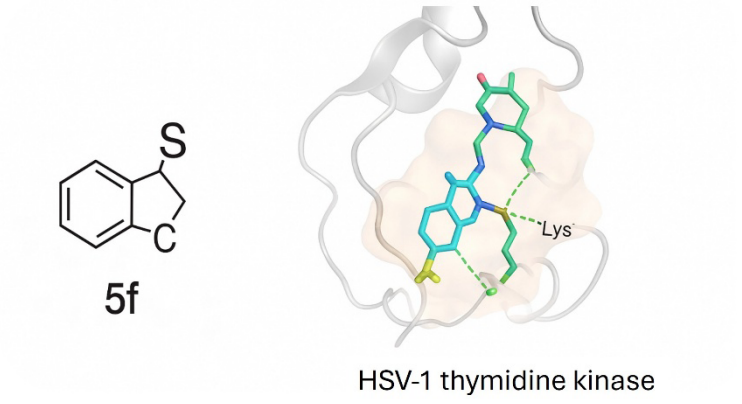

Figure 6. Molecular docking of compound 5f with the herpes simplex virus type 1 (HSV-1) target

potency, the abrupt nature of its response suggests a narrower therapeutic span relative to compounds 5f and 5t.

Taken together, these graphical profiles enhance the transparency of the antiviral analysis and enable a more nuanced interpretation of potency, selectivity, and curve quality.

Figure 7 illustrates the concentration-dependent inhibition of HSV-1 and corroborates the EC_{50} and IC_{50} values reported in Table 4. The curves also highlight differences in curve shape,[24] reproducibility, and therapeutic window among the top-performing compounds. Their inclusion enhances the transparency of the antiviral evaluation and strengthens the overall robustness of the findings.

Table 8. Molecular docking results of compounds 5f, 5t, 5k, and 5a against herpes simplex virus type 1 DNA polymerase

Compound	Docking Score (kcal/mol)	Remarks
5f	−8.7	Best polymerase binder
5t	−8.4	Strong binder
5k	−7.9	Moderate
5a	−7.2	Weak
Acyclovir triphosphate (active form)	−9.5	Expected strong binding

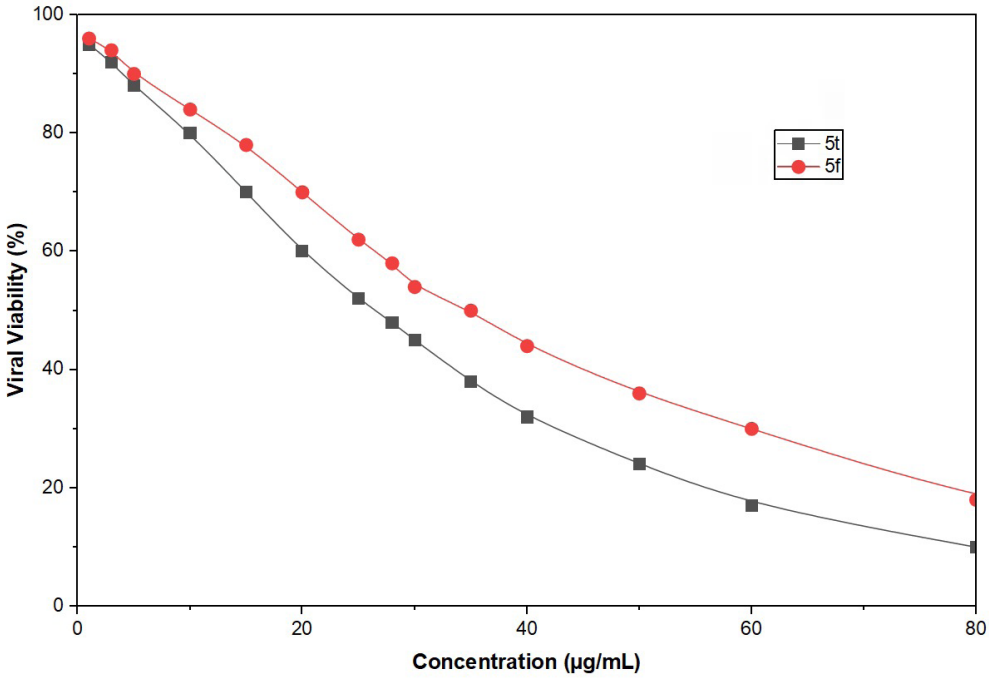

Figure 7. Concentration-dependent inhibition curves of compounds 5f and 5t against herpes simplex virus type 1, showing sigmoidal dose–response relationships and corresponding antiviral activity

4. Conclusion

The test compound's anti-inflammatory, antioxidant, physicochemical, and anti-HSV–1 properties were systematically evaluated in this study, demonstrating its diverse therapeutic potential. With a 68.4% decrease in paw oedema at a dosage of 100 mg/kg, the compound exhibited strong anti-inflammatory efficacy and approached the 72.1% inhibition observed with the standard reference drug. The antioxidant activity demonstrated strong free radical scavenging capacity, suggesting potential utility in mitigating oxidative stress.

Physicochemical profiling provided supporting evidence for its drug development potential by confirming

drug-like properties, including appropriate structural features and solubility. In addition, previously reported *in vitro* anti-HSV studies demonstrated potent antiviral activity, suggesting potential application in antiviral therapy.

Although these findings are promising, minor variations in experimental results may be attributed to experimental variability, including differences in sample preparation, measurement, and procedural execution. Overall, the compound shows potential for further development as an antiviral, antioxidant, and anti-inflammatory agent, pending additional preclinical investigation.

Acknowledgments

We sincerely thank all the members of DB lab for critically reading the manuscript and providing their feedback. AB acknowledges support from the DST National Postdoctoral Fellowship in Nanoscience and Technology. We sincerely thank Ehaa Earth Pvt. Ltd., Mumbai, Thakur College of Engineering and Technology, Mumbai, IIT Gandhinagar, and Pandit Deendayal Energy University, Gandhinagar for providing the necessary facilities to conduct the experiments.

Funding

This study was funded by the Department of Science and Technology Nano Mission, Government of India [grant number: JNC/AO/A.1707/(15)/24-OW-230] and Gujarat State Biotechnology Mission, Government of Gujarat, India [grant number: GSBTM/JD(R&D)/663/2023-24/02003699].

Conflict of interest

The authors declare no conflicts of interest.

Author contributions

Conceptualization: Kiran K. Sanap, Dhiraj Bhatia
Formal analysis: Neha U. Mishra, Kiran K. Sanap
Investigation: Neha U. Mishra, Kiran K. Sanap, Pritesh C. Sharma, Tulsiram Kudale, Jyoti Vanawe, Abhijit Biswas
Methodology: Neha U. Mishra1, Pritesh C. Sharma1, Tulshiram Kudale, Jyoti Vanawe,
Resources: Dhiraj Bhatia
Supervision: Kiran K. Sanap, Abhijit Biswas, Dhiraj Bhatia
Validation: Neha U. Mishra, Pritesh C. Sharma, Tulsiram Kudale, Jyoti Vanawe, Abhijit Biswas
Visualization: Neha U. Mishra, Kiran K. Sanap, Abhijit Biswas
Writing–original draft: Neha U. Mishra, Kiran K. Sanap, Abhijit Biswas
Writing–review & editing: Kiran K. Sanap, Dhiraj Bhatia, Abhijit Biswas

Ethics approval and consent to participate

Not applicable.

Consent for publication

Not applicable.

Availability of data

Data is available from the corresponding author upon reasonable request.

References

1. Nicola AV, Hou J, Major EO, *et al.* Herpes simplex virus type 1 enters human epidermal keratinocytes, but not neurons, via a pH-dependent endocytic pathway. *J Virol.* 2005;79(12):7609-7616.

   doi: 10.1128/JVI.79.12.7609-7616.2005

2. Milne RSB, Nicola AV, Whitbeck JC, *et al.* Glycoprotein D receptor-dependent, low-pH-independent endocytic entry of herpes simplex virus type 1. *J Virol.* 2005;79(11):6655-6663.

   doi: 10.1128/JVI.79.11.6655-6663.2005

3. Montgomery RI, Warner MS, Lum BJ, *et al.* Herpes simplex virus-1 entry into cells mediated by a novel member of the TNF/NGF receptor family. *Cell.* 1996;87(3):427-436.

   doi: 10.1016/S0092-8674(00)81363-X

4. Roizman B, Knipe DM, Whitley RJ. Herpes simplex viruses. In: Knipe DM, Howley PM, eds. *Fields Virology*. 5th ed. Philadelphia, PA: Lippincott Williams & Wilkins; 2007:2501-2601.

5. Piret J, Boivin G. Antiviral resistance in herpes simplex virus and varicella-zoster virus infections: diagnosis and management. *Curr Opin Infect Dis.* 2016;29(6):654-662.

   doi: 10.1097/QCO.0000000000000288

6. Anighoro A, Bajorath J, Rastelli G. Polypharmacology: challenges and opportunities in drug discovery. *J Med Chem.* 2014;57(19):7874-7887.

   doi: 10.1021/jm5006463

7. Saag MS, Benson CA, Gandhi RT, *et al.* Antiretroviral drugs for treatment and prevention of HIV infection in adults: 2018 recommendations of the International Antiviral Society–USA Panel. *JAMA.* 2018;320(4):379.

   doi: 10.1001/jama.2018.8431.

8. Campadelli-Fiume G, Cocchi F, Menotti L, Lopez M. The

novel receptors that mediate the entry of herpes simplex viruses and animal alphaviruses into cells. *Rev Med Virol*. 2000;10(5):305-319.

doi: 10.1002/1099-1654(200009/10)10:5<305::AID-RMV286>3.0.CO;2-T

9. Baranowski E, Ruiz-Jarabo CM, Pariente N, *et al.* Evolution of Cell Recognition by Viruses: A Source of Biological Novelty with Medical Implications. In: *Advances in Virus Research*. Amsterdam: Elsevier; 2003:19-111.

   doi: 10.1016/s0065-3527(03)62002-6

10. James C, Harfouche M, Welton NJ, *et al.* Herpes simplex virus: global infection prevalence and incidence estimates, 2016. *Bull World Health Organ*. 2020;98(5):315-329.

    doi: 10.2471/BLT.19.237149

11. Shukla D, Liu J, Blaiklock P, *et al.* A novel role for 3-O-sulfated heparan sulfate in herpes simplex virus 1 entry. *Cell*. 1999;99(1):13-22.

    doi: 10.1016/S0092-8674(00)80058-6

12. Trottier B, Lake JE, Logue K, *et al.* Dolutegravir/abacavir/lamivudine versus current ART in virally suppressed patients (STRIIVING): a 48- week, randomized, non-inferiority, open-label, Phase IIIb study. *Antivir Ther*. 2016;22(4):295-305.

    doi: 10.3851/IMP3166

13. Spear PG, Eisenberg RJ, Cohen GH. Three classes of cell surface receptors for alphavirus entry. *Virology*. 2000;275(1):1-8.

    doi: 10.1006/viro.2000.0529

14. Gain C, Song S, Angtuaco T, *et al.* The role of oxidative stress in the pathogenesis of infections with coronaviruses. *Front Microbiol*. 2023;13.

    doi: 10.3389/fmicb.2022.1111930

15. Hannah BP, Heldwein EE, Bender FC, *et al.* Mutational evidence of internal fusion loops in herpes simplex virus glycoprotein B. *J Virol*. 2007;81(9):4858-4865.

    doi: 10.1128/JVI.02755-06

16. Chavan H, Shirodkar P, Mogal R, *et al.* Synthesis and evaluation of 1,2,4-triazole derivatives as antimicrobial, antifungal and anthelmintic agents. *Indian J Chem*. 2022;61(9):994-998.

    doi: 10.56042/ijc.v61i9.66354

17. Heldwein EE, Lou H, Bender FC, *et al.* Crystal structure of glycoprotein B from herpes simplex virus 1. *Science*. 2006;313(5784):217-220.

    doi: 10.1126/science.1126548

18. Connolly SA, Jackson JO, Jardetzky TS, *et al.* Fusing structure and function: a structural view of the herpesvirus entry machinery. *Nat Rev Microbiol*. 2011;9(5):369-381.

    doi: 10.1038/nrmicro2548

19. Döhner K, Wolfstein A, Prank U, *et al.* Function of dynein and dynactin in herpes simplex virus capsid transport. *MBoC*. 2002;13(8):2795-2809.

    doi: 10.1091/mbc.01-07-0348

20. Zoete V, Daina A, Bovigny C, *et al.* SwissSimilarity: a web tool for low to ultra high throughput ligand-based virtual screening. *J Chem Inf Model*. 2016;56(8):1399-1404.

    doi: 10.1021/acs.jcim.6b00174

21. Naik S, Puttachari D, Vanishree L, *et al.* Synthesis and biological evaluation of novel hybrid compounds bearing pyrazine and 1,2,4-triazole analogues as potent antitubercular agents. *RSC Pharmaceutics*. 2024;1:283-295.

    doi: 10.1039/D3PM00054K

22. Hu Z, Dong H, Si Z, *et al.* Synthesis and Antibacterial Activity of Novel Triazolo[4,3-a]pyrazine Derivatives. *Molecules*. 2023;28(23):7876.

    doi: 10.3390/molecules28237876

23. Shiraguppi SV, Koganole P, Honnalli SS. A review on 1,2,4-triazoles as scaffold for various pharmacological activities. *J Pharma Insights Res*. 2025;3(3):020-027.

    doi: 10.69613/aewrja40

24. Pintea BN, Panțîr VG, Badea V, *et al.* Pyrazolo [5,1-c] [1,2,4] triazole: a promising emerging biologically active scaffold in medicinal chemistry. *IJMS*. 2025;26(17):8190.

    doi: 10.3390/ijms26178190